Journal of Sound and Vibration (1999) **225**(1), 61–78
Article No. jsvi.1999.2227, available online at http://www.idealibrary.com on IDEAL®

DISCRETE HUYGENS' MODEL APPROACH TO SOUND WAVE PROPAGATION—REVERBERATION IN A ROOM, SOUND SOURCE IDENTIFICATION AND TOMOGRAPHY IN TIME REVERSAL

Y. KAGAWA, T. TSUCHIYA, K. FUJIOKA† AND M. TAKEUCHI‡

Department of Electrical and Electronic Engineering, Okayama University,
3-1-1 *Tsushima-naka, Okayama* 700-8530, *Japan*

(*Received* 10 *March* 1998, *and in final form* 10 *February* 1999)

This is a companion paper to our previous discrete Huyens' model approach to sound wave propagation. The validity and capability of the discrete Huygens' model or transmission-line modelling for the acoustical problems are discussed with applied examples. The acoustical response in a room for which the reverberation is characterized is simulated and a time-reversal approach to sound source identification and acoustic tomography technique is proposed. Some demonstrations are presented.

1. INTRODUCTION

In our previous paper [1], we discussed the fundamental concept and the transmission line matrix approach as a discrete Huygens' modelling. The transmission-line matrix (TLM) modelling is an alternative to the Huygens' modelling, in which electrical impulse scattering are traced on a transmission-line network. In the present paper, we discuss the validity and capability of the modelling by presenting applied examples, the first being the simulation of the sound behaviour in a room. The modelling is also valid when the direction of the time is reversed. With this nature being provided, the application is extended to the identification of the sound source location and intensity based on the measured data observed at the locations surrounding the sources, and also to the identification of an object shape from the response data observed at the locations surrounding it when a certain emanation is made. The work presented here has partly been presented as a lecture (invited) at the International Symposium, Visualization and Auralization for Acoustic Research and Education (ASVA97') [2]. One of the authors has pointed out in a previous paper the potential of the present approach to acoustical problems [3, 4]. Since then, however, there have been papers few published [5, 6] along this line, to the best of the authors' knowledge.

†Presently at Nippon Telegraph and Telephone Corporation, Chugoku-branch, Hiroshima, Japan.
‡Presently at Sharp Corporation, Osaka, Japan.

0022-460X/99/310061 + 18 $30.00/0

Transmission-line matrix modelling was originally developed by Johns and Beurle [7, 8] to solve electromagnetic wave problems. The method was then extensively developed for that purpose, which was well described in the literature [9–12]. The explanation of the process of the discrete Huygens' modelling is possible without referring to the equivalent electrical circuit network by knowing the equivalent pressure and the volume velocity continuity at the node in acoustical network. Acousticians have preferred to use equivalent electrical circuit networks for the acoustical analysis so that the use of the transmission-lines is not foreign to them. One particular feature of the method is that the network is solved in discrete time domain to the impulse excitation, which provides the full wave analysis.

2. SOUND REVERBERATION IN A ROOM [13]

2.1. A THREE-DIMENSIONAL TLM ELEMENT

We discussed a two-dimensional TLM element with which a minute square field is equivalently replaced by a crossed pair of lines or crossed transmission lines of short length [1]. Other short lines can also be added to this for a minute cubic space $\Delta v = (\Delta l)^3$ to create a three-dimensional acoustic element as shown in Figure 1. The transmission lines are simply expressed with six arms connected at the center instead of the four arms for the two-dimensional case. The pulses scattering at the node are illustrated in Figure 2. The mechanism of the scattering at the node when an impulse is entered into arm 1 (characteristic impedance $Z_0 = \rho c$) is similar to the case of the two-dimensional modelling. To the arm 1, the remaining five arms are connected at the node in parallel so that their total impedance is $Z_0/5$, while the impedance in the arm 1 is Z_0. The reflection coefficient Γ at the node is given by

$$\Gamma = \frac{Z_0/5 - Z_0}{Z_0/5 + Z_0} = -\frac{2}{3} \tag{1}$$

so that the impulse of the amplitude $S^1 = (-2/3)P^1$ is reflected back to the arm 1, while the impulses of the amplitude $1/3\,P^1$ each goes through to the other remaining

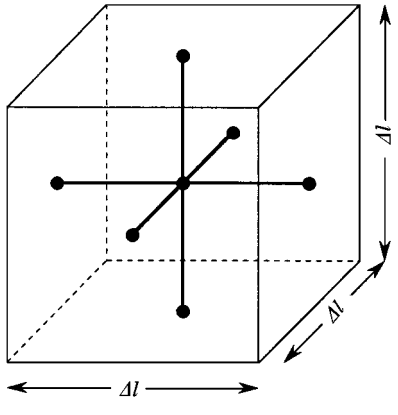

Figure 1. A cubic element and TLM.

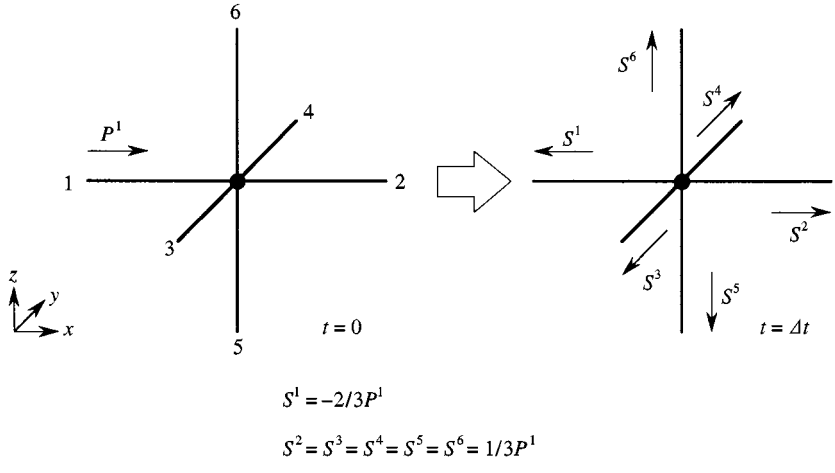

Figure 2. Pulse scattering at the node for a coming impulse.

arms. It takes time $\Delta t (= \Delta l/c$ where c is the propagation speed in free space) for an impulse to be transmitted from the end of one arm to the end of another arm. When the impulses P^i arrive at six arms at time $t = k\Delta t$ $(k = 1, 2, 3, \dots,)$, the reflected sound pressure S^1 at arm 1 at $t = (k + 1)\Delta t$ is given by

$$ {}_{k+1}S^1 = \tfrac{1}{3}({}_kP^2 + {}_kP^3 + {}_kP^4 + {}_kP^5 + {}_kP^6 - 2{}_kP^1). \tag{2} $$

The same happens for all other arms, so that the scattering matrix expression is given by

$$ {}_{k+1}\begin{bmatrix} S^1 \\ S^2 \\ S^3 \\ S^4 \\ S^5 \\ S^6 \end{bmatrix} = \frac{1}{3}\begin{bmatrix} -2 & 1 & 1 & 1 & 1 & 1 \\ 1 & -2 & 1 & 1 & 1 & 1 \\ 1 & 1 & -2 & 1 & 1 & 1 \\ 1 & 1 & 1 & -2 & 1 & 1 \\ 1 & 1 & 1 & 1 & -2 & 1 \\ 1 & 1 & 1 & 1 & 1 & -2 \end{bmatrix}_k \begin{bmatrix} P^1 \\ P^2 \\ P^3 \\ P^4 \\ P^5 \\ P^6 \end{bmatrix}. \tag{3} $$

The pressure $P_{i,j}$ at the node is evaluated as

$$ {}_kP_{i,j} = \frac{1}{3}\sum_{n=1}^{6} {}_kP^n. \tag{4} $$

The field of interest is divided into cubic elements or meshes, in which each cube corresponds to the above element.

The scattered pulses then become the input pulses to the adjacent elements. The sequence of this process creates the propagation of the waves that corresponds to the Huygens' principle, as the field consists of the connection of the elements

forming a network. A wave made of a train of impulses propagates the distance $\Delta l = c_T \Delta t$ for the time Δt. c_T is the propagation velocity in the network which is $c_T = c/\sqrt{3}$. The process can easily be implemented on the computer.

It is sometimes required to evaluate the acoustic energy density in a certain place in the field. The kinetic energy W_1 for a minute volume Δv is defined by

$$W_1 = \tfrac{1}{2}\rho \mathbf{u}^2 \Delta v, \tag{5}$$

where $\mathbf{u}(= \{u_x, u_y, u_z\})$ is the particle velocity (vector), u_x is the x directional component of $\mathbf{u}$ and ρ is the medium density, and the square $\mathbf{u}^2$ means the operation $\mathbf{u}^{\mathrm{T}}\mathbf{u}$. The potential energy is also defined by

$$W_2 = \frac{1}{2}\frac{p^2}{\kappa}\Delta v = \frac{1}{2}\frac{p^2}{\rho c^2}\Delta v, \tag{6}$$

where p is the pressure and κ is the volume elasticity. Therefore, the acoustic energy in the minute volume is

$$W = W_1 + W_2 = \left(\frac{1}{2}\rho u^2 + \frac{1}{2}\frac{p^2}{\rho c^2}\right)\Delta v, \tag{7}$$

where p and u_i correspond, respectively, to

$$p = \frac{1}{3}\sum_{n=1}^{6} P^n,$$

$$u_x = \frac{P^1 - P^2}{\rho c_T}, \qquad u_y = \frac{P^3 - P^4}{\rho c_T}, \qquad u_z = \frac{P^5 - P^6}{\rho c_T}. \tag{8}$$

Thus, the energy density $W/\Delta v$ at the instantaneous time as the wave propagates can easily be evaluated.

2.2. WALL CONDITION AND REFLECTIONLESS BOUNDARY

On the boundary in which the wall impedance of normal incidence Z_w is defined, the reflection coefficient is given by

$$\Gamma = \frac{Z_w - Z_0}{Z_w + Z_0}, \tag{9}$$

where $Z_0 = \rho c_T$. The corresponding condition where the reflection is taking place is

$${}_{k+1}P^1_{i,j} = \Gamma_k S^1_{i,j}, \tag{10}$$

To be non-reflective for simulating outer infinite domain, Z_w is replaced by ρc. Therefore, the reflectionless boundary condition is

$$_{k+1}P^1_{i,j} = \frac{1-\sqrt{3}}{1+\sqrt{3}}\,{}_kS^1_{i,j}. \tag{11}$$

2.3. REVERBERATION IN A ROOM

Using the modelling presented in the previous sections, it is easy to simulate the physical characteristic in a room. The reverberation time is one of the most important figures to characterize the acoustic behaviour in a room, which is relevant to the rate of the energy dissipation, and is defined by the time in which the pressure in a room decays into 1/1000th after the sound source is terminated. The most well-known formula for this are the ones given by Sabine [14] and Eyring [15], which are valid under certain conditions when an ergodic state is possible and determined depending on the volume of the room, the average absorption coefficient and the surface area of the wall.

Here we consider a cubic room whose volume is $(50\Delta l)^3$ as shown in Figure 3, which consists of 125,000 elements. The wall is supposed to have the average sound absorption coefficient $\bar{\alpha}$, which is the sound absorption coefficient averaged with respect to the incident angle to the wall, and is one-half of the normal incident sound absorption coefficient ($\bar{\alpha} = \frac{1}{2}\alpha$ and $\alpha = 1 - R^2$, where R is the reflection coefficient of the wall for normal incidence). In the present simulation, to achieve the condition somewhat similar to being ergodic or diffused, impulses are applied to all the elements until the energy density distribution becomes almost uniform

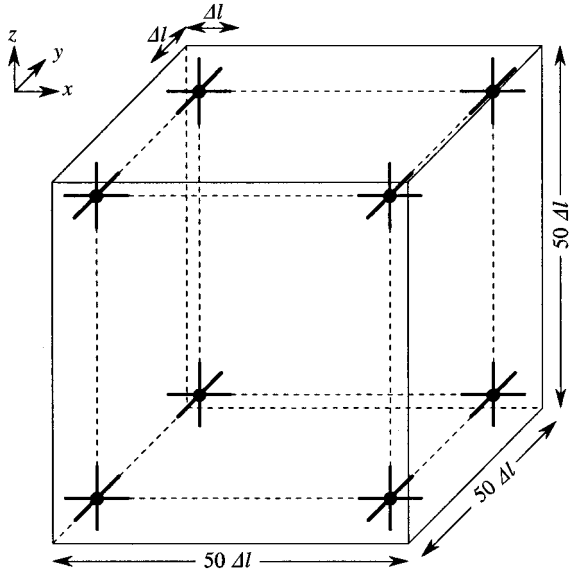

Figure 3. A cubic room.

within a room before the excitation is removed and the sound energy decays. The reverberation time is evaluated from the decay rate, that is, the exponential decay curve, or the slope in the logarithmic scale.

Figure 4 shows an example of the decaying pressure waveform at a certain point of the room. The decay of the energy for various wall conditions of some sound absorption coefficient are given in Figure 5, in which the ordinate is given in logarithmic scale while the abscissas are measured in terms of unit Δt. The reverberation time is obtained from their slopes, which is shown in Figure 6. The results evaluated from the simulation is compared with the values obtained from Sabine's and Eyring's formula. The present result agrees with Eyring's, which is reasonable as Eyring's formula is derived from the consideration of the multireflections with the mean-free-path, while the energy diffusion is only considered in the Sabine's formula. Examination is then extended to the room of irregular shape. The results are shown in Figure 7, in which the simulated results again agree with Eyring's. In the above simulation the sound absorption coefficient is assumed to be independent of the frequency. In reality, the sound absorption

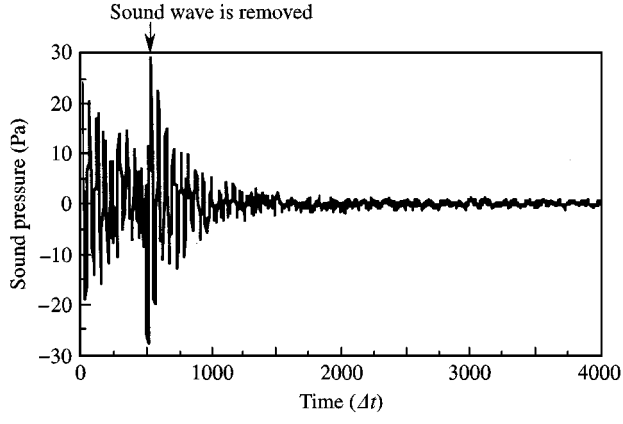

Figure 4. Decaying sound pressure waveform (sound absorption coefficient $\bar{\alpha} = 0{\cdot}1$ at $(25\Delta l, 25\Delta l, 25\Delta l)$)

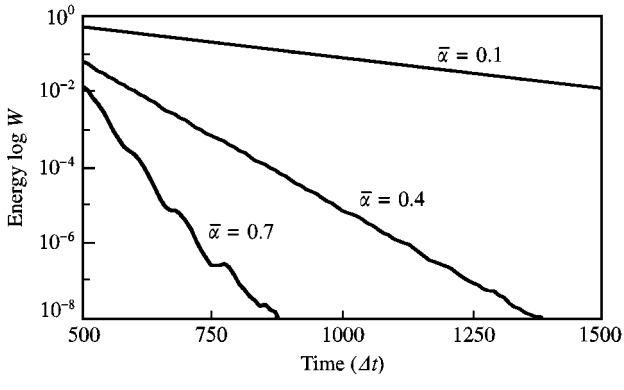

Figure 5. Decaying of the energy with time.

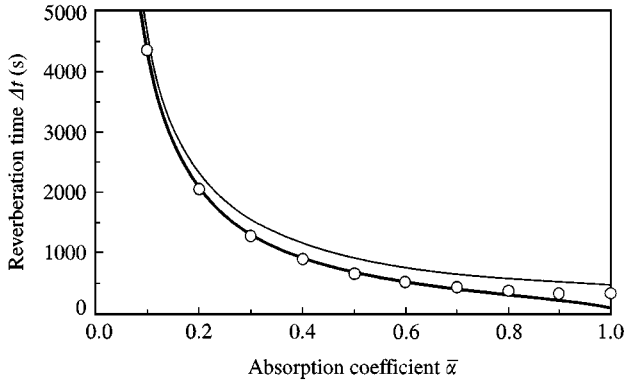

Figure 6. Reverberation time (a cubic room). Key: ——, Eyring; ——, Sabine; ○, present simulation.

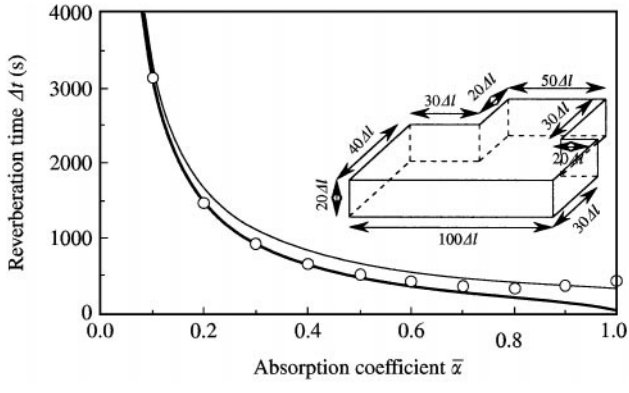

Figure 7. Reverberation time (an irregular room). Key: ——, Eyring; ——, Sabine; ○, present simulation.

coefficient depends on the frequency, which will be reported later in a separate paper. As discussed in our previous paper [1], the accuracy and the computational time required in this method are almost the same as the FD-TD method, but the importance of the TLM modelling is that the physical phenomenon is honestly traced on the computer while FD-TD method is the mathematical method which solves the differential equation numerically. The advantage of the TLM approach will be highlighted in the subsequent section.

3. SOURCE IDENTIFICATION [16]

3.1. PROCESS IN TIME REVERSAL

Here we start by considering a two-dimensional field problem, which has been discussed in our companion paper [1]. The time-reversal process is something like operating a movie film in reverse direction in which the waves propagating outwards from a source again go back to the original source point. This mechanism could be used for source identification problems. The scattering matrix for

a two-dimensional TLM element is

$$_{k+1}\begin{bmatrix} S^1 \\ S^2 \\ S^3 \\ S^4 \end{bmatrix} = \frac{1}{2}\begin{bmatrix} -1 & 1 & 1 & 1 \\ 1 & -1 & 1 & 1 \\ 1 & 1 & -1 & 1 \\ 1 & 1 & 1 & -1 \end{bmatrix}_k \begin{bmatrix} P^1 \\ P^2 \\ P^3 \\ P^4 \end{bmatrix} \tag{12}$$

or

$$_{k+1}\{S\} = [A]_k\{P\}. \tag{13}$$

Multiplying $[A]^{-1}$ on both sides, we have

$$_k\{P\} = [A]_{k+1}\{S\} \tag{14}$$

since

$$[A]^{-1} = [A]. \tag{15}$$

This is the time-reversal process. It is interesting to note that the algorithm is exactly the same for both the forward and the backward process. This mechanism is depicted in Figure 8 for the scattering and concentration in terms of energy. The time-reversal process is also valid for three-dimensional scattering matrix expression. It is easy to perform the time-reversal operation as the TLM method is a physical model. For electromagnetic problems inverse source and inverse scattering problems have been discussed [17].

Noise source identification where the noises come from is of practical importance for noise diagnosis. In the following we discuss an approach to this issue.

3.2. SOUND SOURCE IDENTIFICATION—TWO-DIMENSIONAL FIELD

3.2.1. The case when sound source plane is known

Here we are to identify the sound source field distribution over a certain source plane from the observed data collected over a surface remote from the source plane.

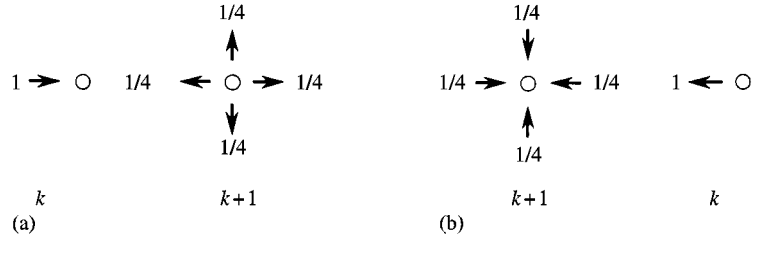

Figure 8. Scattering and concentration in a two-dimensional element (energy). (a) Incident and radiated impulses; (b) time-reversed impulses.

We take a two-dimensional acoustic field as shown in Figure 9. To simulate the free space, non-reflective boundary is created over the boundary that surrounds the field of interest. The data or waveforms are observed or recorded along the surface shown in the figure, from which the sound source distribution is to be recovered through the inverse propagation process. In the present simulation, the solution of the forward problem obtained for the excitation at the sound source location is used for "the observation data". The sound source is set along the line $x = 2$, whose amplitude distribution is assumed to be Gaussian and rectangular. The excitation is a train of 64 impulses with a period of sine wave envelope, for which the data are recorded at each possible position Δl apart along the observation surface. The sound source parameters are tabulated in Table 1. The observed waveforms are then used as the excitation with the time reversed and back propagation is made. The waves are to go back to the original location. The results are observed over the plane $x = 2$. The waveforms are transformed into frequency domain through FFT. The amplitude distribution is obtained for each frequency spectrum. Figure 10 shows the identified results, which are compared with the original sources. Next is the case of plural sources with two different frequencies. The source distribution is as shown in Figure 11(a), consisting of two frequencies. The sound sources used are tabulated in Table 2. The simulation procedure is the same as in the previous example in which the responses recorded over the boundary in the forward solution are used as the excitation sources. The identified source

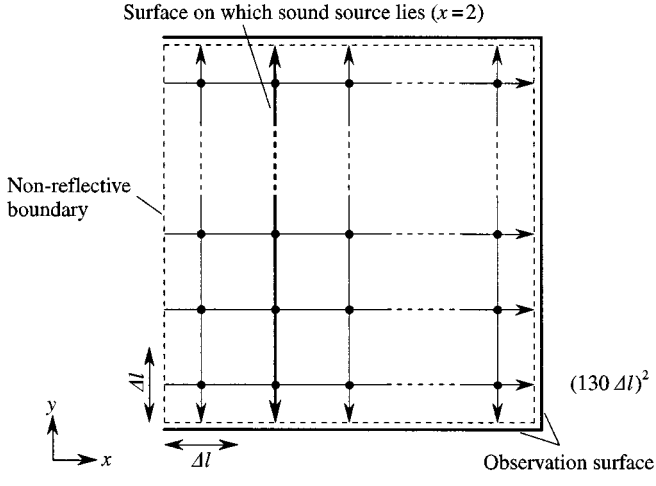

Figure 9. Two-dimensional acoustic field.

TABLE 1

Sound sources

Distribution	Wavelength	Source width
Rectangular	$8\Delta l$	$64\Delta l$ (8λ)
Gaussian	$8\Delta l$	$48\Delta l$ (6λ)

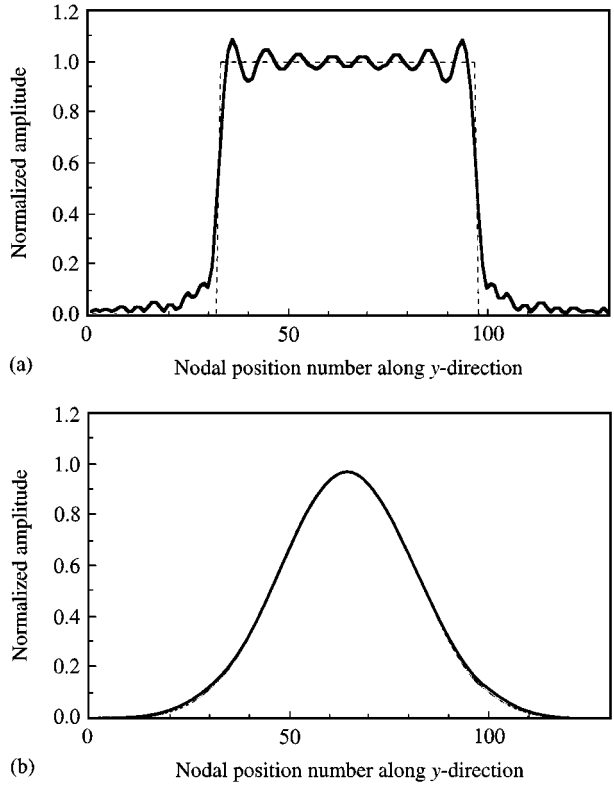

Figure 10. Sound source distributions identified. (a) Rectangular source, (b) Gaussian source. Key: - - -, original; ——, reconstructed.

distributions are, respectively, given in (b) and (c). In the above simulation, data used for the inversion are obtained at locations separated by $\Delta l(=\lambda/8)$. The cases with a smaller number of observation points are examined. The cases where observation points are taken as far as $\lambda/4$, $\lambda/2$, λ and 2λ apart are considered. The results identified are given in Figure 12, in which the identification definitely fails when the interval is wider than the wavelength.

3.2.2. *The case when the sound source plane is unknown*

Here we discuss the case of point sources, as the distributed source consists of point sources. The two-dimensional acoustic field to be considered here is shown in Figure 13, in which the observation is made of all surfaces around the sound sources. The responses for the forward propagation are again used for the sources for the reverse propagation. The power (the square of the sound pressure, time-averaged) at each node is taken over the space. First we consider the case of a single point source made of impulse train in which one is the continuous sine wave (18 periods) and the other is a period of the sine wave. The sources used are tabulated in Table 3. The time-averaged power distributions are shown in Figure 14. The position identified meet the original one. Second, the case of the two point

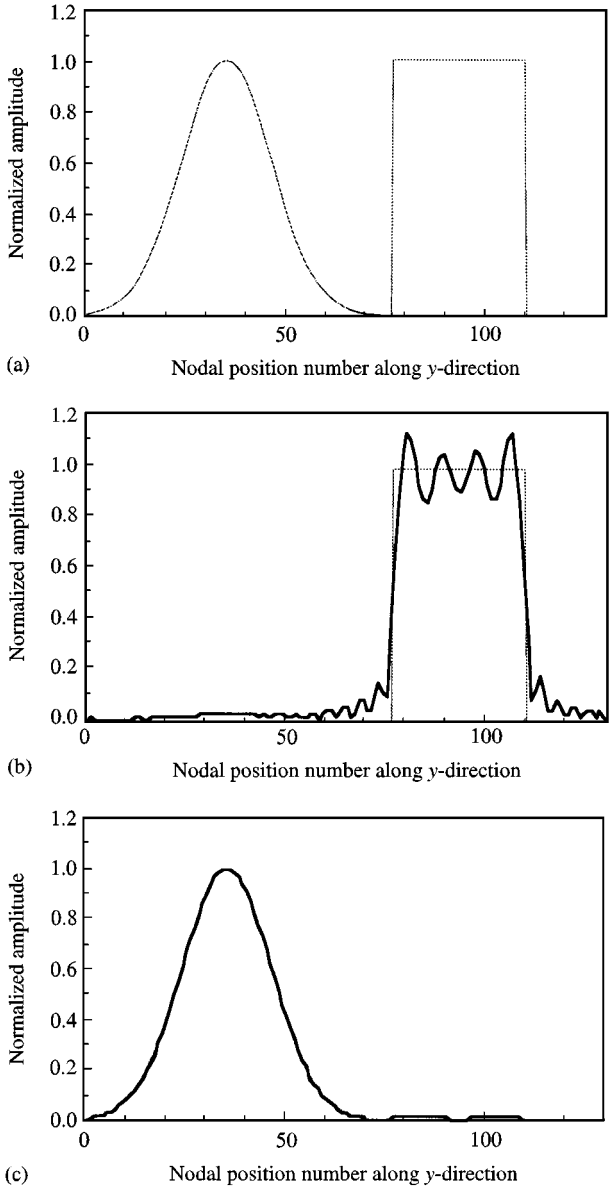

Figure 11. Sound source distributions identified. (a) Original source distribution; (b) rectangular source; (c) Gaussian source. Key: ---, original; ——, reconstructed.

TABLE 2
Sound sources

Distribution	Wavelength	Source width
Rectangular	$8\Delta l$	$32\Delta l$ (4λ)
Gaussian	$16\Delta l$	$32\Delta l$ (2λ)

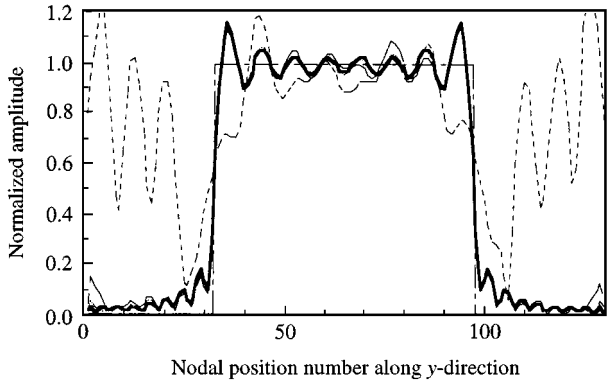

Figure 12. Identified results for different observation point intervals. Key: —·—, original. Reconstructed: ——, $\lambda/8$; ——, $\lambda/4$; ····. $\lambda/2$; – – –, λ; - - - -, 2λ.

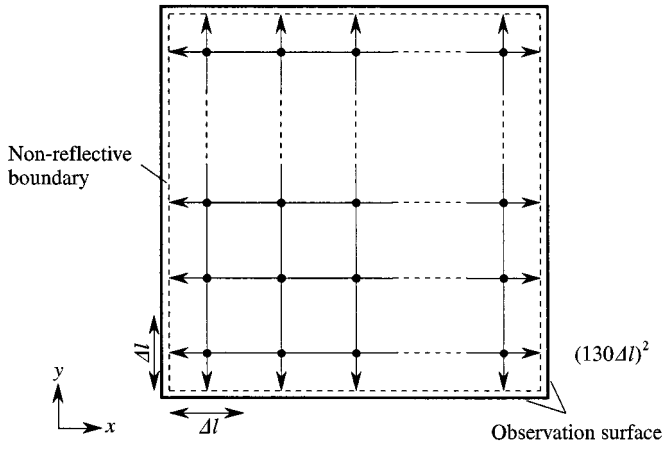

Figure 13. Two-dimensional acoustic field.

TABLE 3
Sound sources

Excitation	Wavelength	Source position	Duration
Continuous wave	$8\Delta l$	(30, 40)	$0T \sim 18T$
A period of sine wave	$8\Delta l$	(30, 40)	$3T \sim 4T$

Note: T: period ($= \lambda/c$)

sources with different frequencies is considered. The acoustic field to be considered is the same as shown in Figure 13. The sources are tabulated in Table 4. The identified results are depicted in Figure 15. For both cases, the two source positions are well identified.

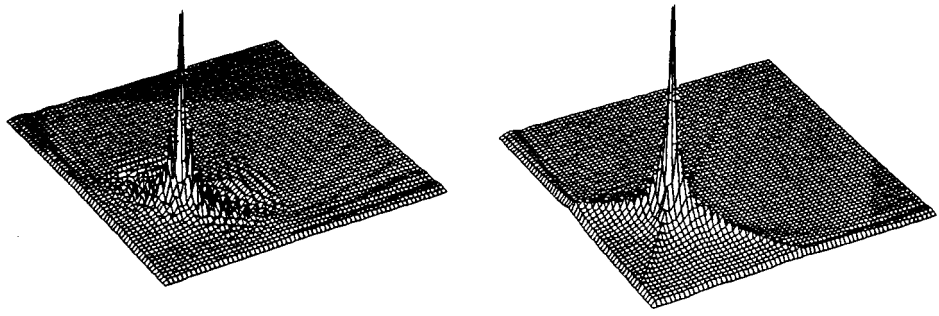

Figure 14. A point source identified.

TABLE 4
Sound sources

Excitation		Wavelength	Source position	Duration
Continuous wave	(1)	$8\Delta l$	(30, 40)	$0T_1 \sim 18T_1$
	(2)	$12\Delta l$	(90, 90)	$0T_2 \sim 12T_2$
A period of sine wave	(1)	$8\Delta l$	(30, 40)	$3T_1 \sim 4T_1$
	(2)	$12\Delta l$	(90, 90)	$3T_2 \sim 4T_2$

Note: T_i: period of source (i)

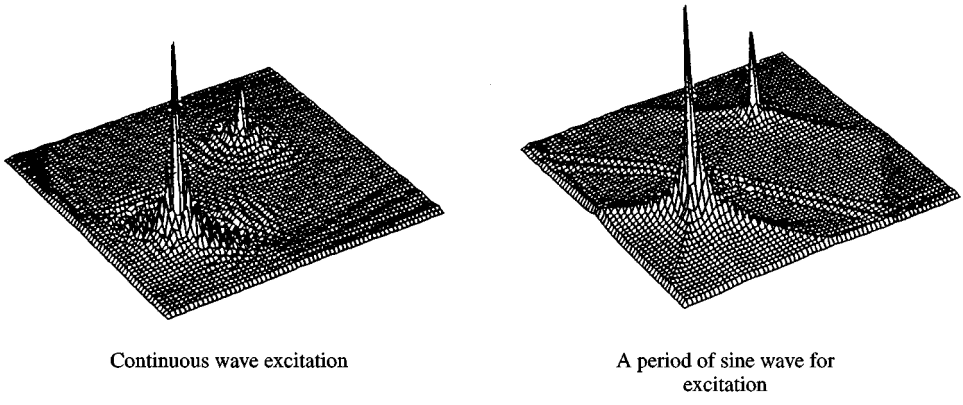

Figure 15. Two point sources identified.

3.3. SOUND SOURCE IDENTIFICATION—A THREE DIMENSIONAL FIELD

Here we consider the source identification in a three-dimensional field. The scattering matrix expression is also valid in time reversal as discussed. The scattering of an impulse and the concentration of the reflected pulses in time

reversal are illustrated for the pressure in Figure 16. For the identification simulation, we take the three-dimensional field as shown in Figure 17, in which the boundary is treated as reflectionless to simulate an unbounded field, and the observation points are provided there. Two-point sources are again considered. The source condition is tabulated in Table 5. Sources are assumed to be on the plane $x = x_0$. The observed data are again used as the sources for the back propagation. The time-averaged square of the pressure is evaluated at every node. The results identified are depicted in Figure 18. The identification is again properly made.

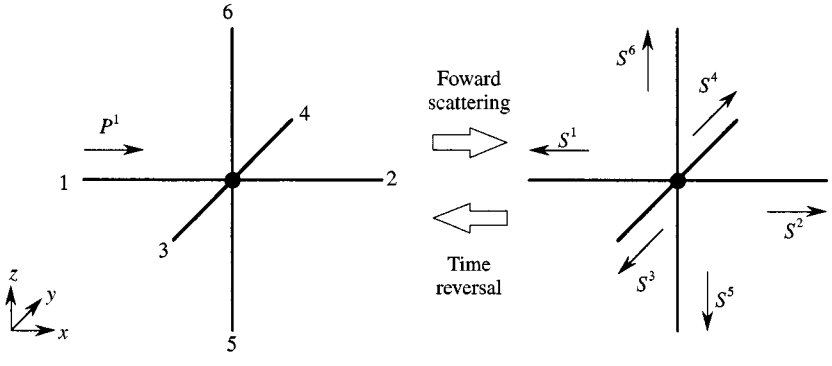

Figure 16. The scattering of a pulse and the concentration of the scattered pulses (in a three-dimensional element).

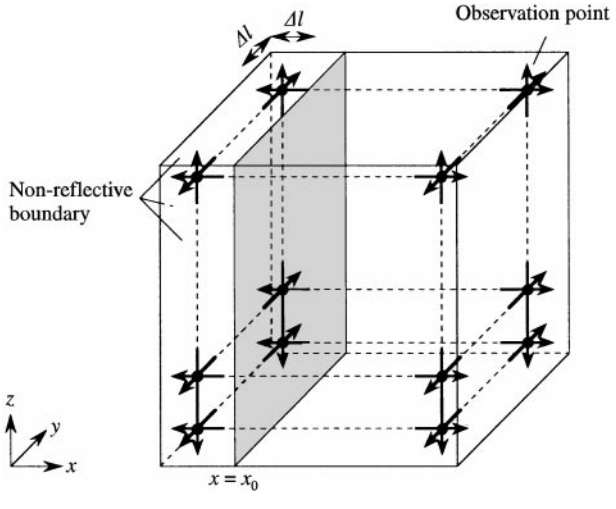

Figure 17. A three-dimensional acoustic field.

TABLE 5
Sound sources

Excitation		Wavelength	Source position	Duration
Continuous wave	(1)	$8\Delta l$	(2, 10, 10)	$0T_1 \sim 18T_1$
	(2)	$12\Delta l$	(2, 35, 35)	$0T_2 \sim 12T_2$
A period of sine wave	(1)	$8\Delta l$	(2, 10, 10)	$3T_1 \sim 4T_1$
	(2)	$12\Delta l$	(2, 35, 35)	$3T_2 \sim 4T_2$

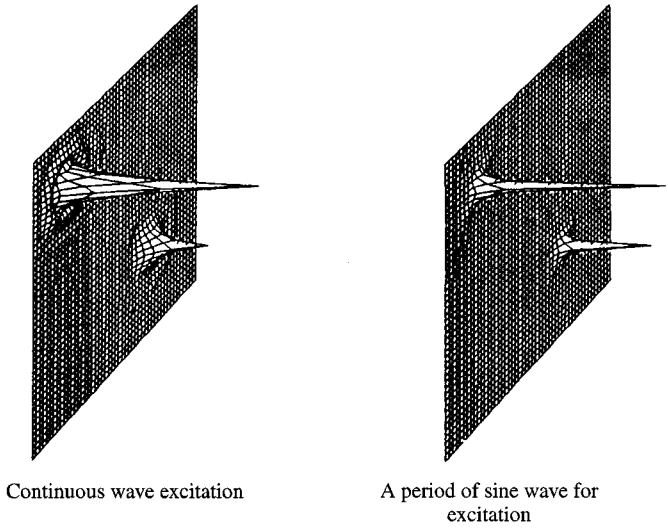

Figure 18. The point sources identified ($x = x_0$).

4. SCATTERING TOMOGRAPHY IN TIME REVERSAL [18]

4.1. PRINCIPLE

Here we again consider a two-dimensional field modelling. In the previous examination, we find that when the measured responses are used as the input they come back to the original source point in the TLM field with a time-reversal process. When an object is illuminated by a certain wave, scattering occurs at the object boundary of different impedance which can be the origin of secondary wave sources. Therefore, a similar process to the one in the source identification described above is practiced with the emanation wave provided. The measured data used as the input in the time reversal process go back to the secondary sources, which leads to the visualization of the object. This is the mechanism of the scattering tomography in time reversal. It is sometimes required to remove the effect of the primary source to ensure a better S/N ratio.

4.2. THE PROCEDURE AND THE EXAMPLE

To prove the principle of the approach proposed, the demonstration is presented here. The simulation consists of the following five steps.

1. *Forward propagation*: Instead of obtaining "the measured data" the scattered data over the region boundary are obtained for the simulation purpose.
2. *Forward propagation*: Data over the region boundary are obtained when no object is placed in the vacant TLM field for collecting the reference data.
3. *Back propagation*: The "measured data" that is obtained by the simulation in Step 1 are used as the input and the responses are observed at every node in the field. The time-averaged energy density distribution is calculated for each node in the space.
4. *Back propagation*: The reference data obtained in Step 2 are used as the input to calculate the time-averaged energy density distribution in the vacant field.
5. *Object reconstruction*: Substraction of the energy density distribution in Step 4 from the energy distribution in Step 3 visualizes the object boundary.

As in many of the computed tomography, we consider here a two-dimensional field for the cross-section of the object. Figure 19 shows the object whose density is 10% higher than the ambient medium. The area under consideration is $(100\Delta l)^2$. Figure 20 (a) shows the reconstructed image or time-averaged power distribution difference when a single Gaussian wave (effective wavelength $8\Delta l$) is used for

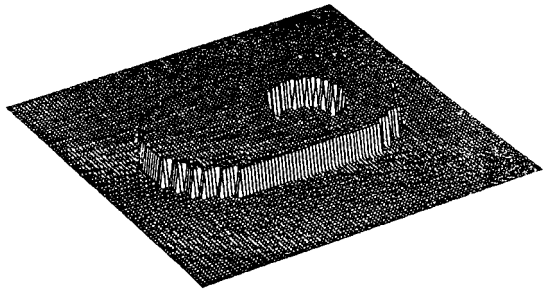

Figure 19. Original object.

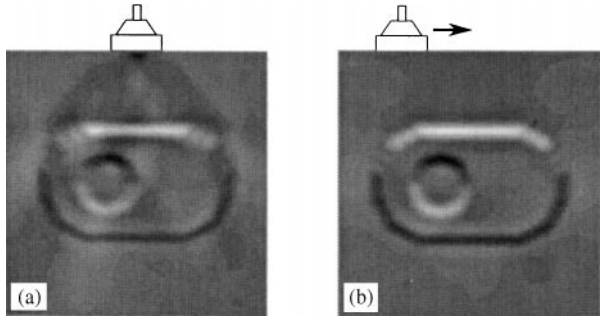

Figure 20. Reconstructed. (a) One-point excitation; (b) one-point but spatially swept excitation.

excitation. The image quality increases when the figures obtained for different excitation positions are superposed, as shown in Figure 20(b). The observation or measurement is made at every Δl interval along the absorbing boundary. If the observation points are separated at intervals greater than the wavelength, the quality of the reconstructed image may deteriorate. For reasonable reconstruction, signal-to-noise ratio more than 60 dB is required for a single excitation.

5. CONCLUDING REMARKS

The potential of the application of the discrete Huygens' modelling or the transmission-line matrix modelling to some acoustical problems have been considered and demonstrated. The acoustical response in a room for which the reverberation is characterized, and a novel approach to sound source identification and acoustic tomography technique in time reversal have been proposed. The validity and capability are discussed with simulated examples. The discussion can be extended to sound absorbing material or a field made of lossy medium with arbitary propagation velocity. These problems will be reported in a separate paper to follow.

REFERENCES

1. Y. Kagawa, T. Tsuchiya, B. Fujii and K. Fujioka 1998 *Journal of Sound and Vibration* **218**, 419–444. Discrete Huygens' model approach to sound wave propagation.
2. Y. Kagawa 1997 *Proceedings of International Symposium, Visualized and Auralization for Acoustic Research and Education* (*ASVA '97*), April, 19–26. Computational acoustics—theories of numerical analysis in acoustics with emphasis on transmission-line matrix modelling (invited).
3. Y. Yoshii, T. Yamabuchi, Y. Kagawa 1976 *Proceeding of the Spring Meeting Acoustical Society Japan* **3–5–10**, 421–422. An application of transmission-line matrix method to acoustical field problems (in Japanese).
4. Y. Yoshii (supervisor: Y. Kagawa) 1977 *M.Sc. Thesis, Toyama University, Japan.* Acoustic field analysis by TLM method (in Japanese).
5. A. H. M. Saleh and P. Blanchfield 1990 *International Journal of Numerical Modelling, Electronic Networks, Devices and Fields* **3**, 39–56. Analysis of acoustic radiation patterns of array transducers using the TLM method.
6. S. El-Masri, X. Pelorson, P. Saguet and P. Badin 1998 *International Journal of Numerical Modelling, Electronic Networks, Devices and Fields* **11**, 133–151. Development of the transmission line matrix method in acoustic applications to higher modes in the vocal tract and other complex ducts.
7. P. B. Johns and R. L. Beurle 1971 *Proceedings of the Institute of Electronics and Engineering* **118**, 1203–1208. Numerical solution of 2-dimensional scattering problems using a transmission-line matrix.
8. P. B. Johns 1974 *IEEE Transactions of the Microwave Theory and Techniques* **MTT-22**, 209–215. The solution of inhomogeneous waveguide problems using a transmission-line matrix.
9. W. J. R. Hoefer 1985 *IEEE Transactions of the Microwave Theory and Techniques* **MTT-33**, 882–893. The transmission-line matrix method—Theory and applications.
10. C. Christopoulos 1995 *IEEE Press.* The transmission—line modeling method.
11. M. N. O. Sadiku and L. C. Agba 1990 *IEEE Transactions of the Circuits and Systems* **CAS-37**, 991–999. A simple introduction to the transmission-line modeling.

12. Directed by Wolfgang J. R. Hoefer and R. Vahldieck 1977 *Workshop Digest of the* 1*st International Workshop on Transmission Line Matrix* (*TLM*) *Modelling—Theory and Applications. Victoria, Canada.*
13. M. Takeuchi, Y. Kagawa and T. Tsuchiya 1996, *Proceedings of the* 17*th Computational Electromagnetics and Electronics, Japan Society of Simulation Technology, December* **11–17**, 193–196. Reverberation sound field simulation in a room using transmission line matrix (TLM) models.
14. W. C. Sabine 1922 *Havard University Press, Cambridge.* Collected papers on acoustics.
15. C. F. Eyring 1930 *Journal of Acoustical Society of America* **1**, 217–241. Reverberation time in dead rooms.
16. K. Fujioka, Y. Kagawa, T. Tsuchiya and T. Furukawa 1995 *Proceedings of the* 16*th Computational Electromagnetics and Electronics, Japan Society of Simulation Technology, December* **I-13**, 61–64. Sound source identification through inverse propagation in a TLM model—simulation.
17. Y. Kagawa and M. Analoui 1994 *Second International Workshop on Finite Element Methods for Electromagnetic Wave Problems, COMPEL May* **13** (Suppl. A), 271–276. Application of TLM model to an inverse problem—identification of source and scatterer in time domain.
18. Y. Kagawa 1996 *Proceedings of Spring Convention, Japanese Acoustical Society*, March **1-9-17**, 913–96. Huygens in computer age–TLM models and their application to acoustic field simulation. (invited).